Computation of Transonic Aerodynamically Compensating Pitot Tube

Shijun Luo* and Yun Bao†
Northwestern Polytechnical University, Xi'an, China

The transonic flows around an aerodynamically compensating pitot tube mounted in front of the fuselage with nose inlet working at various mass flow rates are computed by using the transonic small transverse perturbation equation. The boundary condition and the solution on the body are treated according to the slender-body theory. The successive line over relaxation of the difference equation is accelerated by an artificial time-damping term. The computational results agree well with the wind-tunnel and flight test data.

Introduction

A SIMPLE pitot tube having static pressure orifices located on its cylindrical portion usually cannot obtain the real atmosphere pressure at the flight altitude due to the disturbance induced by the airplane body on which it is mounted. This interference may bring about significant errors in the indication of velocity, Mach number, and pressure altitude (say, an error in pressure altitude of $\Delta H = 300$ m). In order to eliminate these errors, the aerodynamically compensating pitot tube has the static pressure orifices located on the curved meridian such that the disturbance pressure induced by the airplane body is just compensated. There is experimental research on this problem.[1] The present paper deals with the computational aspect.

The pitot tube mounted in front of the fuselage with nose inlet is considered (Fig. 1). There are papers computing the transonic flows about thin bodies of revolution.[2,3] However, as the nose inlet may induce large longitudinal perturbation velocity in front of the fuselage, the classical transonic small perturbation equation (TSP) used by the mentioned papers is not applicable. In this paper, the transonic small transverse perturbation equation (TSTP)[4] is employed. The general properties of the TSTP equation are discussed and compared with those of the TSP equation. To simulate the effects of the inlet on the external flow, the boundary condition on the entrance plane of inlet is established. The boundary condition of the body of revolution is transferred to a cylindrical surface as done by Boppe[3]; however, the solution on the body is interpolated in a more rigorous manner. The artificial time-damping term is introduced in the successive line overrelaxation (SLOR) of the TSTP difference equation, and its effects are obtained by the linearized analyses.

As the influence of the pitot tube on the fuselage is negligible and the region of interest is far from the fuselage, the perturbation pressure of the pitot tube and fuselage combination may be obtained by superposing those of the isolated pitot tube and the isolated fuselage. All these techniques are verified by experiments in the numerical examples.

Governing Equations

The flow around a fuselage with nose inlet may be assumed a small transverse perturbation. Under this assumption, the perturbation potential equation in cylindrical coordinates (x,r,θ) is the TSTP equation[4]

$$(1-M^2)\phi_{xx}+\phi_{rr}+\phi_r/r+\phi_{\theta\theta}/r^2=0 \tag{1}$$

where

$$1-M^2=\frac{1-M_\infty^2-\dfrac{\gamma+1}{q_\infty}M_\infty^2\phi_x-\dfrac{\gamma+1}{2q_\infty^2}M_\infty^2\phi_x^2}{1-\dfrac{\gamma-1}{q_\infty}M_\infty^2\phi_x-\dfrac{\gamma-1}{2q_\infty^2}M_\infty^2\phi_x^2} \tag{2}$$

and q_∞ and M_∞ are the freestream velocity and Mach number, γ is the ratio of specific heats, and M is the local Mach number. The TSP equation is Eq. (1) with

$$1-M^2=1-M_\infty^2-\frac{\gamma+1}{q_\infty}M_\infty^2\phi_x \tag{3}$$

The TSTP equation is valid for all speeds $0<M_\infty<\infty$, while the TSP equation is not valid for $M_\infty \gg 1$.

The pressure coefficient formula for TSTP is

$$c_p=\frac{2}{\gamma M_\infty^2}\left\{\left[1-(\gamma-1)M_\infty^2\left(\frac{\phi_x}{q_\infty}+\frac{\phi_x^2}{2q_\infty^2}\right)\right]^{\frac{\gamma}{\gamma-1}}-1\right\} \tag{4}$$

As $M=1$, from Eq. (2)

$$\frac{\phi_x}{q_\infty}+\frac{\phi_x^2}{2q_\infty^2}=\frac{1-M_\infty^2}{(\gamma+1)M_\infty^2} \tag{5}$$

Substituting into Eq. (4), the exact critical pressure coefficient is obtained as

$$c_p^*=\frac{2}{\gamma M_\infty^2}\left\{\left[\frac{2}{\gamma+1}\left(1+\frac{\gamma-1}{2}M_\infty^2\right)\right]^{\frac{\gamma}{\gamma-1}}-1\right\} \tag{6}$$

The critical pressure coefficient from TSP is not exact:

$$c_p^*=\frac{2(M_\infty^2-1)}{(\gamma+1)M_\infty^2} \tag{7}$$

The weak oblique shock formula for TSTP flow is

$$\frac{1-M_\infty^2-\dfrac{\gamma+1}{q_\infty}M_\infty^2\dfrac{u_1'+u_2'}{2}-\dfrac{\gamma+1}{2q_\infty^2}M_\infty^2\left(\dfrac{u_1'+u_2'}{2}\right)^2}{1-\dfrac{\gamma-1}{q_\infty}M_\infty^2\dfrac{u_1'+u_2'}{2}-\dfrac{\gamma-1}{2q_\infty^2}M_\infty^2\left(\dfrac{u_1'+u_2'}{2}\right)^2}\times(u_1'-u_2')^2+(v_1'-v_2')^2=0 \tag{8}$$

Presented as Paper 87-2613 at the AIAA 5th Applied Aerodynamics Conference, Monterey, CA, Aug. 17–19, 1987; received June 23, 1987; revised Aug. 20, 1987.

*Professor, Department of Aircraft Engineering; presently, Visiting Professor, Department of Mechanical Engineering, Santa Clara University, Santa Clara, CA.
†Graduate Student.

where (u_1',v_1') and (u_2',v_2') are the perturbation velocity components on the upstream and downstream sides of the shock wave. For a shock wave in the freestream, Eq. (8) reduces to

$$\left[1-M_\infty^2-\frac{\gamma+1}{q_\infty}M_\infty^2\frac{u_2'}{2}-\frac{\gamma+1}{2q_\infty^2}M_\infty^2\left(\frac{u_2'}{2}\right)^2\right]u_2'^2 + \left[1-\frac{\gamma-1}{q_\infty}M_\infty^2\frac{u_2'}{2}-\frac{\gamma-1}{2q_\infty^2}M_\infty^2\left(\frac{u_2'}{2}\right)^2\right]v_2'^2=0 \tag{9}$$

This is the TSTP shock polar at M_∞. The exact and TSP shock polars at M_∞ are, respectively,

$$\left(1-M_\infty^2-\frac{\gamma+1}{q_\infty}M_\infty^2\frac{u_2'}{2}\right)u_2'^2+\left(1-\frac{\gamma-1}{q_\infty}M_\infty^2\frac{u_2'}{2}\right)v_2'^2=0 \tag{10}$$

and

$$\left(1-M_\infty^2-\frac{\gamma+1}{q_\infty}M_\infty^2\frac{u_2'}{2}\right)u_2'^2+v_2'^2=0 \tag{11}$$

Equations (9–11) are plotted in Fig. 2 for $M_\infty=1.2$.

Boundary Conditions

Instead of computing the interior flow of the inlet, a boundary condition on the entrance plane is satisfied:

$$\phi_x=q_i-q_\infty \tag{12}$$

where q_i is the average velocity at the inlet entrance, which may be quite different from q_∞. The boundary condition on the body of revolution, $r=R(x)$, is transferred to a nearby cylindrical surface $r=r_o$, where r_o is assumed constant; i.e.,

$$\phi_r(x,r_o,\theta)=q_\infty R'(x)\frac{R(x)}{r_o}-q_\infty\alpha\frac{R^2(x)}{r_o^2}\cos\theta \tag{13}$$

where α is the angle of attack. In the case of a fuselage with a nose inlet, r_o is taken to be equal to the radius of inlet entrance. Otherwise, r_o is taken to be half of the maximum radius of body.

After the solution is found on $r=r_o$, the perturbation velocity components on the body are interpolated by the slender-body theory:

$$\phi(x,R,\theta)=\phi_x(x,r_o,\theta)\frac{r_o}{R}+q_\infty[R(x)R'(x)]'\ell n\frac{R}{r_o} -\frac{1}{2\pi}\int_0^{2\pi}\phi_x(x,r_o,\theta)\,d\theta\left(\frac{r_o}{R}-1\right) \tag{14}$$

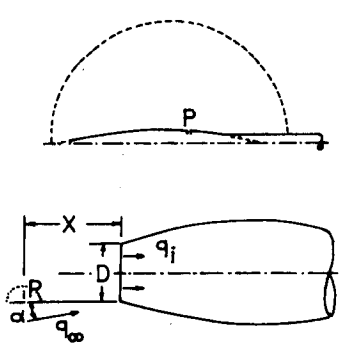

Fig. 1 Compensating pitot tube and fuselage with nose inlet.

and

$$\frac{\phi_\theta(x,R,\theta)}{R(x)}=\frac{\phi_\theta(x,r_o,\theta)}{r_o}\frac{r_o^2}{R^2(x)} \tag{15}$$

Boppe used the Taylor's series expansions for the interpolation, which may be invalid due to the singularities on the body axis $r=0$.

Difference Methods

The Murman-Cole nonconservative difference scheme[5] is used. From a Taylor series expansion to second order, the difference expressions of the first- and second-order derivatives should have the second and first order of accuracy, respectively. The resulting difference equations are solved by SLOR. In the region $r<r_o$, the relaxation line is parallel to the x axis. Elsewhere, the relaxation line is along the radial direction. When M_∞ is close to 1, the preceding algorithm may yield slow convergence and even oscillation. To overcome this difficulty, the artificial time-damping term[6] is introduced into the TSTP equation (1) at locally supersonic points $M>1$:

$$(1-M^2)\phi_{xx}+\phi_{rr}+\frac{\phi_r}{r}+\frac{\phi_{\theta\theta}}{r^2}+\varepsilon\frac{\Delta t}{\Delta x}\phi_{xt}=0 \tag{16}$$

where t is the artificial time variable corresponding to the iteration number n of the SLOR.

The SLOR along the r direction of the difference equation of Eq. (16) for the axisymmetric case is

$$(1-M^2)\frac{\bar\phi_{i,j}^{(n)}-2\phi_{i-1,j}^{(n)}+\phi_{i-2,j}^{(n)}}{\Delta x^2}+\frac{\bar\phi_{i,j+1}^{(n)}-2\bar\phi_{i,j}^{(n)}+\bar\phi_{i,j-1}^{(n)}}{\Delta r^2} +\frac{\bar\phi_{i,j+1}^{(n)}-\bar\phi_{i,j-1}^{(n)}}{2r\,\Delta r}+\varepsilon\frac{\bar\phi_{i,j}^{(n)}-\phi_{i-1,j}^{(n)}-\phi_{i,j}^{(n-1)}+\phi_{i-1,j}^{(n-1)}}{\Delta x^2}=0 \tag{17}$$

where

$$\bar\phi_{i,j}^{(n)}=\frac{1}{\omega}\phi_{i,j}^{(n)}+\left(1-\frac{1}{\omega}\right)\phi_{i,j}^{(n-1)} \tag{18}$$

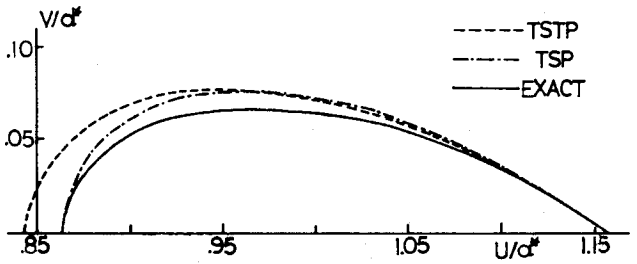

Fig. 2 Shock polar at $M_\infty=1.2$.

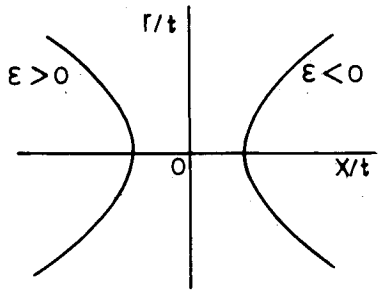

Fig. 3 Characteristics of Eq. (19) for $\omega=1$.

and ω is the relaxation factor. Under the linearization assumption $M = \text{const}$, Eq. (17) is equivalent to the artificial time-dependent differential equation

$$(1-M^2)\phi_{xx} + \phi_{rr} + \frac{\phi_r}{r} + \varepsilon\frac{\Delta t}{\Delta x}\phi_{xt} + a\frac{\phi_{rt}}{r} + b\phi_t = 0 \quad (19)$$

where

$$a = -(1-1/\omega)\,\Delta t \quad (20)$$

$$b = -(1-1/\omega)(1-M^2+\varepsilon)\,\Delta t/\Delta x^2 \quad (21)$$

By the variable transformation

$$\left.\begin{aligned} x &= \xi \\ r &= \eta \\ \tau &= t - \frac{\epsilon\Delta t}{2(1-M^2)\Delta x}x - \frac{a}{2}\ell n r \end{aligned}\right\} \quad (22)$$

Equation (19) can be written in the canonical form

$$(1-M^2)\phi_{\xi\xi} + \phi_{\eta\eta} + \frac{\phi_\eta}{\eta} - \frac{1}{4}\left(\frac{\varepsilon^2\Delta t^2}{(1-M^2)\Delta x^2} + \frac{a^2}{r^2}\right)\phi_{\tau\tau} + b\phi_\tau = 0 \quad (23)$$

Equation (23) is of hyperbolic type. In the limiting case $\tau \to \infty$, ξ is the pseudotime variable. So is ξ in the general case. Hence,

$$\varepsilon^2 > (1-1/\omega)^2(M^2-1)\,\Delta x^2/r^2 \quad (24)$$

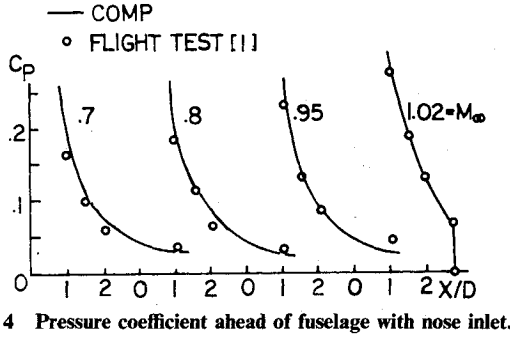

Fig. 4 Pressure coefficient ahead of fuselage with nose inlet.

Therefore, the linearized analysis shows the need of the ϕ_{xt} term. A characteristic of Eq. (19) when $\omega = 1$ is

$$\frac{1}{4}\frac{\varepsilon^2\Delta t^2}{\Delta x^2}\left(\frac{r}{t}\right)^2 = 1 - M^2 - \frac{\varepsilon\,\Delta t}{\Delta x}\frac{x}{t} \quad (25)$$

Equation (25) is plotted in Fig. 3. The characteristics, including the positive x/t axis, should be chosen. Thus,

$$\varepsilon < 0 \quad (26)$$

The numerical results agree with the preceding linearized analyses.

Numerical Examples

The flight test data of the fuselage with a nose inlet[1] is used to verify the present computational method as shown in Fig. 4 for $M_\infty = 0.7$, 0.8, 0.95, and 1.02, $\alpha = 0$, and q_i/q_∞ varying from 0.68 to 0.5 as M_∞ varies from 0.7 to 1.10. The agreement is very good.

A paraboloid of revolution with a fineness ratio of 12 at $M_\infty = 0.9$ and 1.1 and $\alpha = 4$ and 6 deg is computed and confirmed by the known wind-tunnel test results,[7] as shown in Fig. 5. In the computation, the well-known formulas

$$\phi_\theta = (\phi_{i,j,k+1} - \phi_{i,j,k-1})/2\sin\Delta\theta \quad (27)$$

$$\phi_{\theta\theta} = (\phi_{i,j,k+1} - 2\phi_{i,j,k} + \phi_{i,j,k-1})/2(1-\cos\Delta\theta) \quad (28)$$

are used so that $\Delta\theta$ as large as $\pi/4$ yields sufficiently convergent results in numerical experiments.

An aerodynamically compensating pitot tube is shaped by the paraboloid of revolution of fineness ratio 9.091 and has four static pressure orifices located at the section, 65% from the nose tip relative to the total length of the paraboloid, and $\theta = +20$ and ± 142 deg. The computations show that the static pressures at $\theta = \pm 142$ deg are almost independent of α for positive α (Fig. 6). The addition of the orifices at $\theta = \pm 20$ deg is to take care of both positive and negative angles of attack. Figure 7 shows the static pressure coefficients computed and measured in the wind-tunnel test[8] at $M_\infty = 0.4 \sim 1.12$ and $\alpha = 0$ and 8 deg. They agree very well.

The described pitot tube is combined with a fuselage with a nose inlet.[9] It is found that the pressure coefficient produced by the pitot tube does essentially compensate for that produced by the fuselage with a nose inlet. Figure 8 shows that the errors of the pressure altitude indicated by the pitot tube are almost null for $M_\infty = 0.4 \sim 0.92$ and that the agreement between the computation and the flight test[9] is quite good.

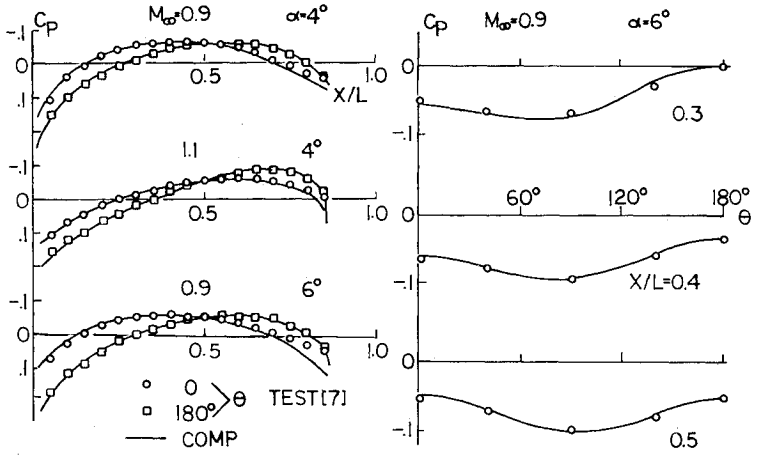

Fig. 5 Pressure coefficient on paraboloid of revolution, fineness ratio 12.

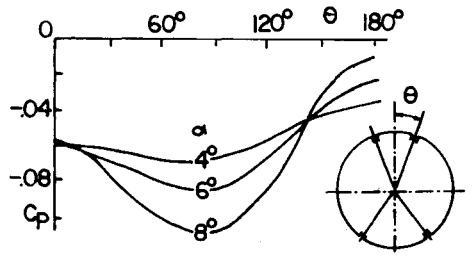

Fig. 6 Circumferential pressure distribution of pitot tube.

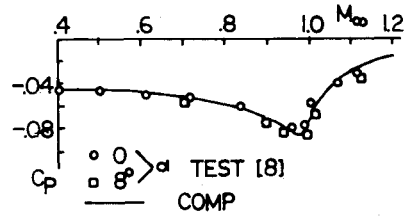

Fig. 7 Pressure coefficient of compensating pitot tube.

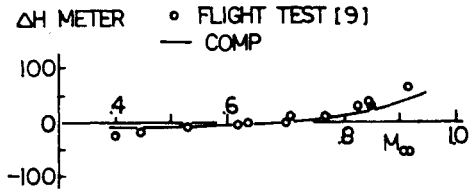

Fig. 8 Error of pressure altitude indicated by compensating pitot tube.

Conclusions

The TSTP equation is applicable to the flow around the inlet. Besides, it yields the exact critical pressure coefficient and the approximate shock wave relation. The increase in computer time relative to the TSP equation is negligible. The transfer of the boundary condition on the body as well as the interpolation of the solution to the body are treated uniquely through the slender-body theory in the present paper. The recognition of the pseudotime variable and the significant characteristics of the linearized artificial time-dependent partial-differential equation does yield some guidance to the actual computation.

References

[1]O'Bryan, T. C., Danforth, E. C. B., and Johnston, J. F., "Error in Airspeed Measurement due to the Static Pressure Field Ahead of an Airplane at Transonic Speeds," NACA Rept. 1239, 1955.

[2]Stahara, S. S. and Spreiter, J. R., "A Transonic Wind Tunnel Interference Assessment—Axisymmetric Flow," *AIAA Journal*, Vol. 18, Jan. 1980, pp. 63–71.

[3]Boppe, C. W., "Computational Transonic Flow about Realistic Aircraft Configurations," AIAA Paper 78-104, 1978.

[4]Luo, S. J., Zheng, Y. W., Qian, H., and Wang, D. Q., "Finite Difference Computation for Transonic Steady Potential Flows," *Computer Methods in Applied Mechanics and Engineering*, Vol. 27, 1981, pp. 129–138.

[5]Murman, E. M. and Cole, J. D., "Calculation of Plane Steady Transonic Flows," *AIAA Journal*, Vol. 9, 1971, pp. 114–121.

[6]Jameson, A., "Iterative Solution of Transonic Flow over Airfoils and Wings, Including Flow at Mach 1," *Communications on Pure and Applied Mathematics*, Vol. 27, 1974, pp. 283–309.

[7]McDevitt J. B. and Taylor, R. A., "Force and Pressure Measurements at Transonic Speed for Several Bodies Having Elliptical Cross Section," NACA TN 4362, 1958.

[8]Tu, X. and Wu, W. K., "Transonic Wind Tunnel Test of the Compensating Pitot Tube," Aerodynamics Institute, Northwestern Polytechnical University, 1984.

[9]An, C. J., "Flight Test of the Compensating Pitot Tube," First Institute of China Air Force, 1985.